MICROSTRUCTURAL ANALYSIS OF THE COLD WORKING
EFFECT ON THE FRACTURE TOUGHNESS OF WELD METAL
IN HSLA STEEL WELDS

Lj. Nedeljković, A. Radović and S. Sedmak

Faculty of Technology and Metallurgy,
University of Belgrade, Yugoslavia

INTRODUCTION

The effect of cold mechanical working on the mechanical properties
of steel structures, and welded joints, as their critical parts, is
of practical importance for several reasons. Test overstressing,
with the aim of proving the reliability and subsequent performance
of a structure, can produce a slight but tangible amount of plastic
deformation. Accidental overloadings in operation, that can never
be completely excluded, are another potential source of plastic
deformation.

It is usually considered that prior plastic deformation, produced by
test overstressing, beneficially affects the subsequent behaviour
and reliability of a structure (Nichols, 1968; Egan, 1968; Terazawa,
Otani, Ueda, Kihara, 1968).

The results of an investigation into the effect of initial plastic
deformation, developed in the course of test overloading of a
prototype for a hydroelectric power plant penstock, made of HSLA HT80
steel (Sedmak, Radović, Nedeljković, 1979) did not confirm this point
of view. On the contrary, a decrease in the resistance of welded
joints to brittle fracture after initial plastic deformation was
observed. A definite dependence of the ductile/brittle Charpy V
transition of the weld metal on the direction of plastic deformation,
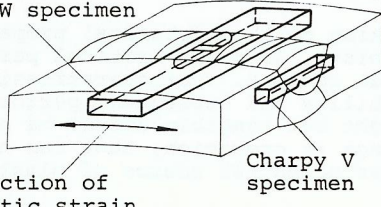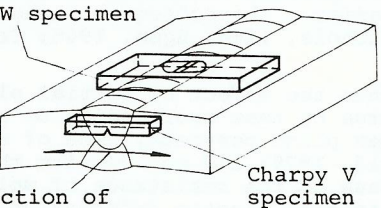relative to the longitudinal welded joint axis, could also be shown.

The purpose of this paper is to try to find some plausible
explanation for the directional effect of plastic deformation on weld
metal resistance to brittle fracture through microstructural
examination and fractographic analysis.

CHANGES IN THE MECHANICAL PROPERTIES OF WELD METAL
AFTER INITIAL PLASTIC DEFORMATION

A cylindrical prototype, 4.2 m in diameter, made of 47 mm thick
SUMITEN 80P steel plates, welded together by 2/3 X manual (MAW) and
submerged arc (SAW) welded joints, was overloaded up to 75% of the
yield point (750 MPa) of base plate steel. In the course of the
prototype test overloading plastic deformations developed in the weld

metal. They were recorded by the strain gauges, placed on the outer side of the prototype, and varied from zero up to about 0.2%, depending on the welded joint position. The previously evidenced differences in the transition temperature, determined on the Charpy V and drop weight specimens cut out from the prototype after straining of about 0.2%, and from trial welds, which were not strained, are summarized in Table 1. Obviously, straining causes a definite increase in the nil ductility temperature (NDT) of all welded joints, relative to undeformed trial welds, independent of both weld type and strain direction.

TABLE 1 Change in a Characteristic Ductile/Brittle Transition Temperature after Initial Plastic Deformation of about 0.2% (Prototype Specimens) relative to Undeformed Welded Joints of the Same Type (Trial Weld Specimens) (Sedmak, Radović, Nedeljković, 1979)

Schematic representation of a main direction relative to welded joint position	Type of welded joint	ΔNDT*	ΔT_{tr}** Charpy V
A. DW specimen Direction of plastic strain / Charpy V specimen	1 SAW circular (specimens: prototype SAW-C7, trial weld 3)	+ 26	+ 4
	2 MAW circular (specimens: prototype MAW-C8, trial weld 4)	+ 3	+ 16
B. DW specimen Direction of plastic strain / Charpy V specimen	3 SAW longitudinal (specimens: prototype SAW-L6, trial weld 2)	+ 11	- 26
	4 MAW longitudinal (specimens: prototype MAW-L5, trial weld 1)	+ 13	- 20

* ΔNDT = NDT$_{strained\ joint}$ - NDT$_{nonstrained\ joint}$

** ΔT_{tr} = $T_{tr,strained\ weld\ metal}$ - $T_{tr,nonstrained\ weld\ metal}$

T_{tr} is determined as the temperature at which the impact energy attains half of the room temperature value.

A sort of directional effect of straining on the mechanical properties is already visible in the drop weight test results for submerged arc welded joints. As shown in the Fracture Analysis Diagrams (Fig. 1a and 1b), pertaining to submerged arc longitudinal and circular welded joints, the plastic deformation in the direction of the welded joint axis adversely affects the nil ductility temperature in a more pronounced way (Table 1, A), than if it is transverse to the welded joint (Table 1, B).

The drop weight test evaluates the behaviour and performance of a welded joint as a whole. The results of total absorbed energy, in impact fracturing of Charpy V notch specimens cut out from weld metal
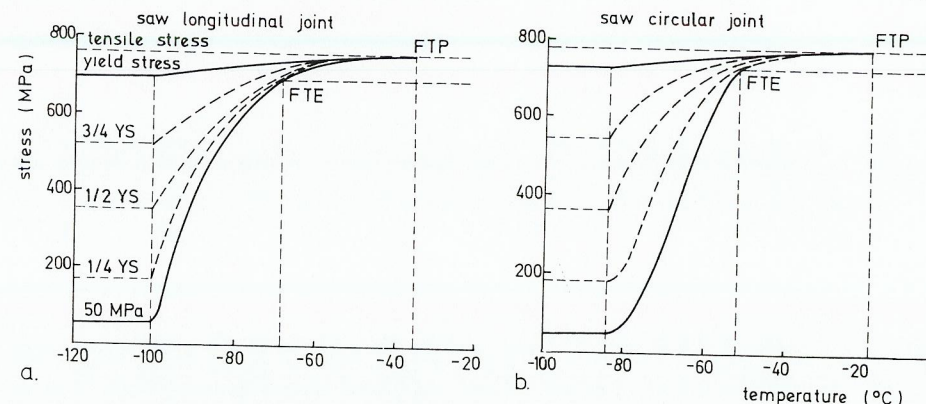
Fig. 1. Fracture Analysis Diagrams for longitudinal L6 (a) and circular C7 (b) submerged arc welded joints after straining
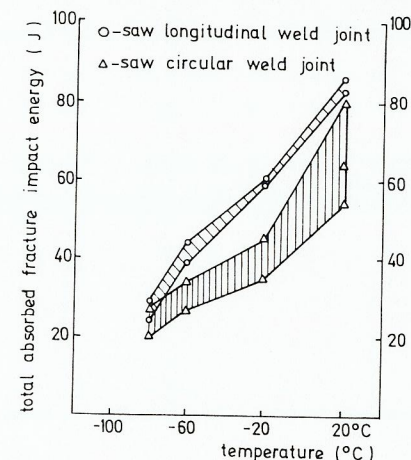

Fig. 2. Dependence of submerged arc weld metal Charpy V impact toughness, after straining, on temperature

after straining, at various temperatures (Fig. 2) illustrate in more detail the dependence of weld metal notch impact properties on the straining direction, summarized in Table 1. The transition temperature for weld metal of a longitudinal submerged arc welded joint, strained transversely to the weld axis and with notch and fracture surface in the weld axis, is decreased with respect to the nonstrained weld metal (Table 1, B). On the contrary, the transition temperature for the weld metal of a circular submerged arc welded joint, strained in the welding direction, is increased with respect to the nonstrained weld metal (Table 1, A). Moreover, all but one of the impact energy values for the weld metal of a longitudinal welded joint lie above that for the weld metal of a circular weld.

In order to make an outline of the possible relations between structural directionality features of a weld metal and the position of a fracture surface, the influence of the notch position on weld metal impact toughness is determined separately. The Charpy V specimens for this determination are cut out from the weld metal of a longitudinal submerged arc welded joint strained about 0.2% (prototype specimen LS4). The macrostructure of the welded joint in two vertical cross sections, normal to one another, is seen in Fig. 3. The position of transverse and longitudinal Charpy V specimens in a weld is presented in Fig. 4, together with the notch locations and microstructure of the corresponding fracture surfaces. The notch impact results in the form of total absorbed energy - temperature scatter ranges, in Fig. 5, show that total absorbed energy values for
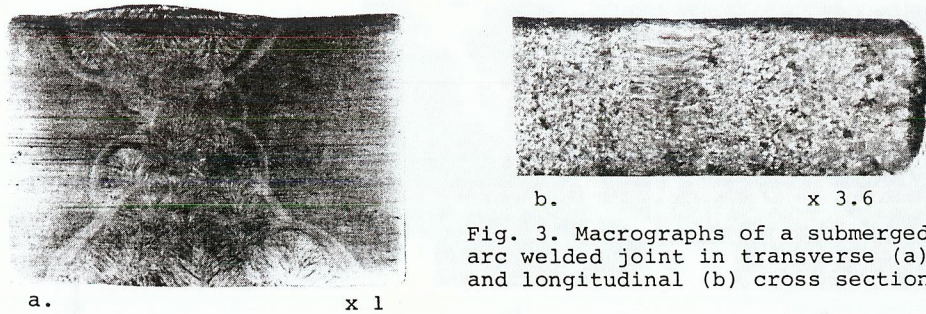
b.   x 3.6

Fig. 3. Macrographs of a submerged arc welded joint in transverse (a) and longitudinal (b) cross section

a.   x 1

x 50

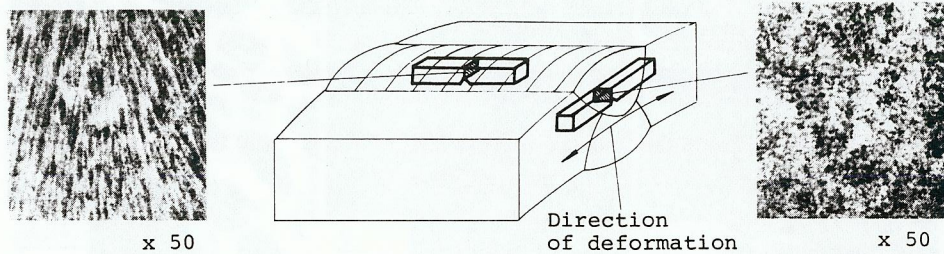Direction of deformation

x 50

Fig. 4. Schematic view of Charpy V specimen position in 0.2% strained longitudinal prototype LS4 submerged arc weld together with location and microstructure of fracture surface

longitudinal specimens, with fracture surfaces in a vertical plane normal to the weld axis, are on average lower than for transverse specimens taken from the same weld metal. Fig. 5 presents the existence of an additional directional effect on the notch impact properties of a weld metal, based in this case solely on weld metal microstructural anisotropy. Together with the effect of cold mechanical working, exhibited in Fig. 2, it underlines the definite directionality of weld metal resistance to fast fracturing.
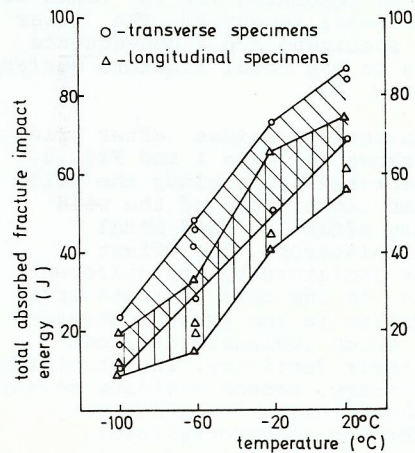

Fig. 5. Dependence on temperature of notch impact toughness of transverse and longitudinal weld metal Charpy V specimens taken from the longitudinal prototype weld LS4

CHEMICAL COMPOSITION AND MICROSTRUCTURAL FEATURES OF THE WELD METALS

The chemical composition of a submerged and manual arc weld metal is given in Table 2.

TABLE 2   Chemical Composition of Weld Metals

Weld metal	C %	Si %	Mn %	P %	S %	Cr %	Ni %	Mo %	Al %	Ti %	O ppm	N ppm
SAW	0.08	0.43	1.98	0.015	0.010	0.57	0.32	0.82	0.022	0.013	582	80
MAW	0.08	0.55	1.51	0.013	0.010	0.43	1.75	0.49	0.013	0.023	342	112

Because of the possible importance for the fracturing behaviour of the weld metal the presence of nonmetallic inclusions is carefully examined. A high oxygen content in weld metal is already an indication of a high oxide inclusion concentration. Microscopic examination at low magnification showed, as illustrated in Fig. 6, a substantially higher inclusion presence in the weld metal than in the base steel plate. The higher density of inclusions in Fig. 6 itself separates the weld metal from the base plate.
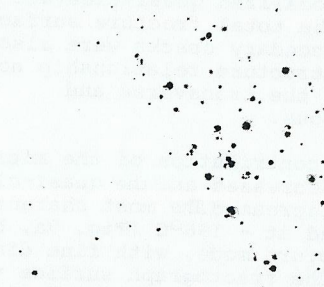

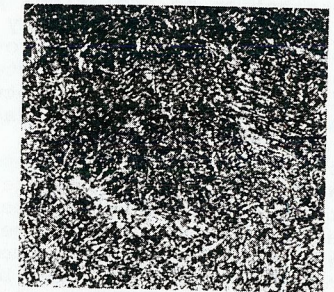Fig. 6. Nonmetallic inclusions in SAW joint   x 100

Fig. 7. Microstructure of SAW weld metal   x 200

An attempt to determine the total volume concentration of inclusions is summarized in Table 3. The results are the fraction occupied by inclusions of the total examined area of a polished specimen, including a record of more than 10,000 observed inclusions each. All inclusions that could be seen at the magnification x 480 were recorded without distinguishing between oxides, sulfides, carbides and possibly nitrides. The next important feature noticed is a very broad size distribution range, starting with a few coarse and ending with a great number of very fine inclusions of microscopically visible and submicroscopic size level.

TABLE 3   Volume Concentration of All Microscopically Visible Inclusions Determined by the Counting Method

Welded joint	Volume Concentration, %	
	Base plate	Weld metal
SAW	0.209	0.572
MAW	0.190	0.266

The microstructure of the submerged arc weld metal in Fig. 7 consists predominantly of proeutectoid ferrite and bainite. Their mutual ratio varies largely over the weld metal cross section and could not be

assessed quantitatively. Grain boundaries of different types are seen in the micrograph. Grain boundaries in the form of black lines, well revealed by deep etching, are an indication of a largely transformed cast structure by interpass annealing. Grain boundaries in the form of black carbide particle rows can be taken as a sign of a nontransformed cast structure. White grain boundaries of a platelike interphase structure are most probably a result of redistribution of segregated elements by interpass annealing, or alternatively might be a consequence of dendritic segregations during solidification.

FRACTOGRAPHIC ANALYSIS

The fracture surfaces of the Charpy V SAW transverse and longitudinal weld metal specimens, fractured at different temperatures are examined with SEM to determine the fracture surface topography and fracture mechanism.

Fracture at 20°C in both transverse and longitudinal specimens occurred by microvoid coalescence, with equiaxed dimples ranging from fine to large (Fig. 8a and b) as a consequence of the broad size distribution of inclusions present. A localized quasi-cleavage mode of rupture contributed very little to the total fracture surface. A small number of large microvoids and secondary cracks were also observed. Neither the fracture - microstructure relationship nor the difference between the rupture modes of the transverse and longitudinal fracture surfaces was obvious.

With a decreasing test temperature the contribution of the microvoid coalescence mode of rupture gradually decreased and the quasi-cleavage with secondary cracks correspondingly increased. The most characteristic fracture surface appearance was observed at - 196°C (Fig. 9a, b and c). The quasi-cleavage is a predominant rupture mode, with fine dimples concentrated in the grain boundaries. The fractograph surface view at low magnification in Fig. 9a and b shows a topography of grain and subgrain boundaries in the form of narrow dimpled areas in the faceted quasi-cleavage matrix. More dimpled grain boundary areas are seen on the fracture surface of the transverse than of the longitudinal Charpy V specimens (Fig. 9a and b, respectively). The view at higher magnification (Fig. 9c) shows the intergranular dimpled areas to be 1 - 5 µm in width.

No evidence of intergranular separation was found in any of the specimens analysed.

DISCUSSION

The results of weld metal ductile/brittle transition in Figs. 2 and 5 show the existence of anisotropy in the fracture toughness of the weld metal, which may be exhibited in various forms in different circumstances.

One type of this anisotropy, as shown in Fig. 5, has its origin in a weld metal microstructural anisotropy. The weld metal microstructure, as seen in Figs. 3 and 4, consists mainly of columnar grains, which are by their principal axis oriented normal to the base plate edges, i.e. the longitudinal welded joint axis, coinciding with a principal direction of heat conduction during solidification.
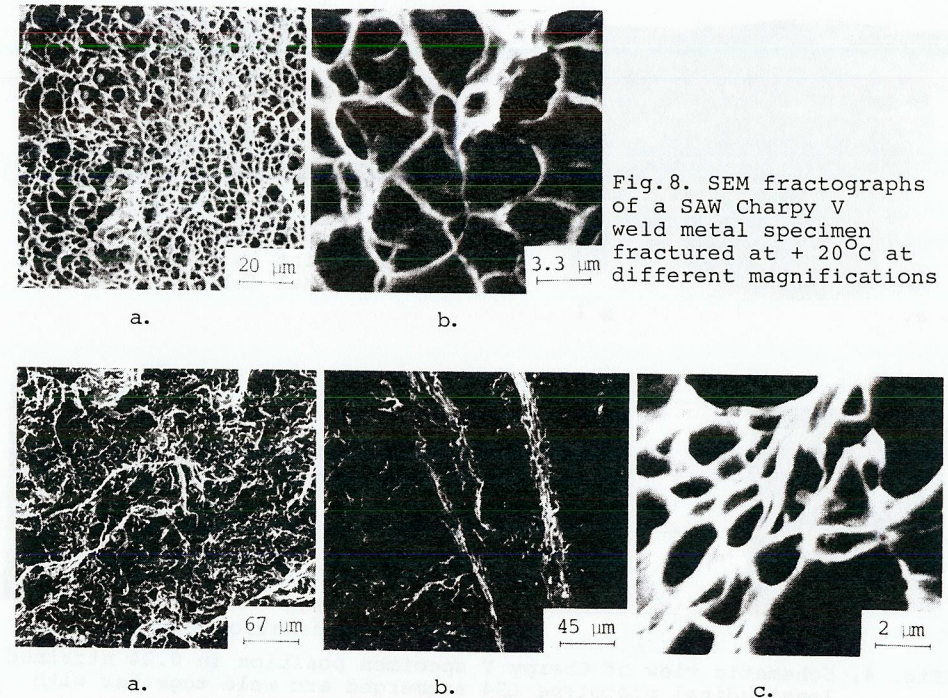
Fig.8. SEM fractographs of a SAW Charpy V weld metal specimen fractured at + 20°C at different magnifications

a.   b.

a.   b.   c.

Fig. 9. SEM fractographs of SAW Charpy V transverse (a) and longitudinal (b), and a detail from grain boundary (c) of weld metal specimens, fractured at - 196°C

The grain boundaries, as shown by fractographic analysis (Fig. 9a, b, c) are the toughest microconstituent in the weld metal microstructure. The toughness anisotropy in Fig. 5 can be accounted for in terms of the grain boundary effect on total weld metal toughness. The lower absorbed energy values of longitudinal specimens are a consequence of a lower grain boundary fraction area in the total fracture surface, relative to the transverse specimens (Fig. 4).

Another type of weld metal toughness anisotropy arises after prior plastic deformation of about 0.2%. As shown in Table 1 and Fig. 2, the straining transverse to the weld decreases, and along the weld increases the ductile/brittle transition temperature of the weld metal. Again, in terms of grain boundary effect on weld metal toughness and of weld metal structural anisotropy, the effect of plastic deformation in two cases may be explained by its different forms, relative to the grain boundaries. In the case of transverse straining the resulting plastic deformation in the grain boundaries occurs predominantly by shear-sliding, which obviously does not impair, and even beneficially affects their ductility. The straining along the welded joint axis, on the contrary, causes yielding mainly normal to the grain boundary planes, which lowers the plasticity reserve of grain boundaries as a reinforcing microconstituent, adversely affecting the toughness of the weld metal as a whole.

The methods used in this investigation were not sensitive enough to enable more detailed elucidation of the micromechanism by which the straining affects the weld metal toughness. Not even the role of different kinds of grain and subgrain boundaries could be accounted for. It remains the task of further investigations by other more sophisticated fine-structural research methods.

The results obtained have as a whole a methodological significance in the field of weld metal testing (Dawes, 1974). They show that in the case of the weld metal examined, with grain boundaries as the most ductile microconstituent, a most critical fracture surface lies in a plane transverse to the welded joint axis. This may be a reason to prescribe the longitudinal Charpy V specimen as decisive in this case for weld metal inspection. With materials of different microstructural characteristics the critical position of the fracture surface could also be different and should be tested in every individual case.

CONCLUSIONS

The effect of straining and microstructural anisotropy on weld metal toughness was investigated. It was shown that two types of weld metal toughness anisotropy exist. With the same weld metal the toughness values are higher when the fracture surface cuts columnar crystals across their principal axis than when it passes along them. The straining transverse to the welded joint axis beneficially affects the weld metal notch impact toughness and the straining along the weld axis impairs it. Fractographic analysis showed the grain boundaries to be the most ductile microconstituent in the weld metal microstructure. The toughness anisotropy observed could be accounted for in terms of grain boundary effect on the behaviour of weld metal as a whole.

The results obtained have methodological significance for weld metal testing. They show that for a type of material with grain boundaries as the most ductile microconstituent, the critical fracture surface lies in a plane transverse to the welded joint axis, and consequently a longitudinal Charpy V specimen should be taken as decisive for weld metal inspection.

ACKNOWLEDGEMENTS

REFERENCES

Dawes, M.G. (1974). Weld. J., 55, Dec. p. 1052.
Egan, G.R. (1968). Welding Institute Research Bulletin, Nr. 9, p. 231.
Nichols, R.W. (1968). British Weld. J., 15, p. 21.
Sedmak, S., Radović, A., Nedeljković, Lj. (1979). Proceedings of ICM 3, Cambridge, England, 3, p. 435.
Terazawa, K., Otani, M., Ueda, I., Kihara, H. (1968). Technol. Rep. Osaka Univ., Nr. 18, p. 583